Numerical Investigation of Thermal Field Characteristics for Turbulent Al_2O_3-Water Nanofluid Flow in a Circular Tube

M.S. Youssef[1,2,*], A-F. Mahrous[1,3], E-S.B. Zeidan[1,4], A. Balabel[1,3] and A.S. Al-Osaimy[1]

[1] Mechanical Engineering Department, College of Engineering, Taif University, Al-Haweiah, PO Box 888, Saudi Arabia

[2] Mechanical Engineering Department, Faculty of Engineering, Assiut University, Assiut PO Box 71516, Egypt

[3] Mechanical Power Engineering Department, Menoufiya University, Shebin-El-Kom, 32511, Egypt

[4] Mechanical Power Engineering Department, Faculty of Engineering, Mansoura University, Mansoura, Egypt

[*]Corresponding Author: (E-mail address youssef2056@yahoo.com, M.S. Youssef)

Abstract

The thermal field characteristics of Al_2O_3-water nanofluid flowing in a circular tube under turbulent flow regime with and without heat transfer were numerically investigated. A single phase fluid model in conjunction with a two-equation turbulence model for hydrodynamic field and a zero-equation model for thermal field was employed to determine the thermal field characteristics of Al_2O_3-water with three nanoparticle volume concentrations. It was revealed from the simulated results that by increasing the volume concentration of nanoparticles, the radial temperature difference was decreased, where the average heat transfer coefficient and the wall shear stress were increased. Furthermore, the predicted results showed that the temperature or wall heat flux had passive effect on the turbulent hydrodynamic field characteristics. Ultimately, with increasing the volume concentration of nanoparticles, the production rate and dissipation rate of turbulent kinetic energy were increased and that is agreed quite well with previous studies.

Key Words: Nanofluids, Numerical Simulation, Turbulent Flow, Thermal Field, Constant Wall Heat Flux

1. Introduction

Nanofluids are created by dispersing nanometer-sized particles in a base fluid such as water, ethylene glycol or propylene glycol. Use of high thermal conductivity metallic nanoparticle such as copper, aluminium, silver and silicon increases the thermal conductivity of such mixtures, thus enhancing their overall energy transport capability. Because of their unique features, nanofluids have attracted attention as a new generation of fluids in building heating, heat exchangers, technological plants, automotive cooling applications and many other applications. By employing nanofluids it is possible to reduce the dimensions of heat transfer equipments, thanks to the increase in the heat transfer efficiency due to the improved thermophysical properties of the working fluid.

Various experimental studies have been carried out to investigate the behavior and heat transfer characteristics of different nanofluids under turbulent flow regime [1-8]. These experimental studies have been performed at small range of particle concentrations, nearly less than 2 % for different kinds of nanoparticles with various nanoparticle diameters. The experimental data obtained in these studies show enhancement in heat transfer parameters such as heat transfer coefficient and Nusselt number with increasing the particle concentrations and decreasing the particle diameter.

Regarding the theoretical/numerical models reviewed, different numerical studies were proposed to study the mechanism of heat transfer by using different nanoparticles with various nanoparticles concentrations [9-15]. The numerical studies of nanofluids can be conducted using either single-phase (homogenous) or two-phase approaches. In the former approach it is assumed that the fluid phase and nanoparticles are in thermal equilibrium with zero relative velocity. While, in the latter approach, base fluid and nanoparticles are considered as two different liquid and solid phases with different momentums respectively [9]. Some of the findings of these studies will be discussed here due to limitation of space. Turbulent flow and heat transfer of three different nanofluids flowing through a circular tube under constant heat flux condition have been numerically analyzed by Namburu et al. [10]. They assumed and used single-phase fluid model to solve two-dimensional steady, forced turbulent convection flow of nanofluid flowing inside a straight circular tube. Two-equation turbulence model of launder and Spalding was adopted by Namburu et al. [10] in their numerical analysis. Their computed results indicated that heat transfer coefficient and pressure loss increase with increase in the volume concentration of nanofluids and Reynolds number. Commercial CFD package, FLUENT, was used by Demir et al. [14] for solving the

volume-averaged continuity, momentum, and energy equations of different nanofluids flowing in a horizontal tube under constant temperature condition. Their numerical results have clearly indicated that the increase in Nusselt number and the heat transfer coefficient by the various nanofluid volume concentrations over the base fluid of pure water. They attributed the increase in heat transfer coefficient to the higher Prandtl number and thermal conductivity of nanopartilces than the base fluid and also a large energy exchange process resulting from the chaotic movement of nanoparticles. They noted also that, Nusselt number and heat transfer coefficient increase with increasing Reynolds number.

To summarize what is reviewed above, it is well-known that the heat transfer performance of nanofluids is significantly better than the traditional working fluids. However, the previous experimental studies with low concentrations of nanoparticles, nearly less than 2 %, have shown that enhancement of the heat transfer performance. Also, different numerical investigations have been carried out and clearly indicated that the increase in Nusselt number and the heat transfer coefficient by the various nanofluid volume concentrations over the base fluid. Therefore, more numerical studies of flowing nanofluids under turbulent flow regime with wider range of nanoparticle concentrations to disclose the heat transfer characteristics are awaited.

In the present proposal, thermal field characteristics of nanofluids in a circular tube under a turbulent flow regime with and without wall heat flux will be studied numerically. Effects of volume concentrations of nanoparticles on the thermal field characteristics are explored and discussed in detail.

2. Flow Governing Equations and Thermophysical Properties

The nanofluid has been treated as incompressible, steady state, homogeneous and Newtonian fluid. The flow has been modelled using Navier-stokes equations using FLUENT 6.3 package solver [16]. The single phase homogeneous flow governing equations in the Cartesian co-ordinates are continuity, momentum, and energy equations and are written, respectively, as follows [17]:

$$\frac{\partial}{\partial x_i}(\rho u_i) = 0 \tag{1}$$

$$\frac{\partial}{\partial x_j}(\rho u_i u_j) = -\frac{\partial P}{\partial x_i} + \rho g_x + \frac{\partial}{\partial x_j}\left[\mu\left(\frac{\partial u_i}{\partial x_j} + \frac{\partial u_j}{\partial x_i}\right)\right] + \frac{\partial}{\partial x_j}\left(-\rho\overline{u_i' u_j'}\right) \tag{2}$$

$$\frac{\partial}{\partial x_j}(\rho u_i T) = \frac{\partial}{\partial x_j}\left(\Gamma\frac{\partial T}{\partial x_j} - \overline{u_j t}\right) \tag{3}$$

In the preceding equations, the last terms in the momentum and energy equations represent the Reynolds shear stress and the turbulent heat flux, respectively, and are need to be modelled.

Using the concept of turbulent viscosity, the Reynolds shear stress in Eq. (2) may be written as:

$$-\rho\overline{u_i' u_j'} = \mu_t \left(\frac{\partial u_i}{\partial x_j} + \frac{\partial u_j}{\partial u_i}\right) \tag{4}$$

The Turbulent viscosity, μ_t, in Eq. (4) is to be computed from an appropriate turbulence model. In the present numerical analysis, a two-equation turbulence model is used to determine the turbulent viscosity and correspondingly the hydrodynamic field characteristics. Among the two-equation turbulence models, the $k-\varepsilon$ model is currently most often used for turbulence predictions [18]. In the $k-\varepsilon$ model, the reference velocity of turbulence is represented by $k^{1/2}$ and the characteristic length scale is given by $L_e = k^{3/2}/\varepsilon$, which is the typical length scale of energy-containing eddies. Therefore, the turbulent viscosity for the $k-\varepsilon$ model may be written as:

$$\mu_t = \rho\, C_\mu k^{1/2} L_e = \rho\, C_\mu \frac{k^2}{\varepsilon} \tag{5}$$

In Eq. (5), the turbulent kinetic energy k and its dissipation rate ε are determined from the following two differential equations [18]:

$$\frac{\partial}{\partial x_i}(\rho k u_i) = \frac{\partial}{\partial x_j}\left[\left(\mu + \frac{\mu_t}{\sigma_k}\right)\frac{\partial k}{\partial x_j}\right] + G_k + \rho\varepsilon \tag{6}$$

$$\frac{\partial}{\partial x_i}(\rho \varepsilon u_i) = \frac{\partial}{\partial x_j}\left[\left(\mu + \frac{\mu_t}{\sigma_\varepsilon}\right)\frac{\partial \varepsilon}{\partial x_j}\right] + C_{\varepsilon 1}\frac{\varepsilon}{k}G_k + C_{\varepsilon 2}\rho\frac{\varepsilon^2}{k} \tag{7}$$

In Eqs. (6 and 7), the production rate of turbulent kinetic energy G_k is determined from the following expression:

$$G_k = -\rho\,\overline{u_i' u_j'}\,\frac{\partial u_i}{\partial x_j} \tag{8}$$

In the above set of equations, the values of the constants are given as follows:

$C_\mu = 0.09,\ \sigma_k = 1.0,\ \sigma_\varepsilon = 1.3,\ C_{\varepsilon 1} = 1.44,\quad C_{\varepsilon 2} = 1.92$

A Temperature field can be analyzed from the energy equation (3). However, this equation is not closed since it contains an unknown turbulent heat flux $\overline{u_j t}$ and, therefore, need to be modelled as mention previously. Using the turbulent diffusivity for heat Γ_t, we represent a turbulent heat flux $-\rho\overline{u_i' u_j'}$ by the following simple gradient form [17]:

$$-\overline{u_j t} = \Gamma_t \frac{\partial T}{\partial x_j} \quad (9)$$

Based on Eq. (9), the energy equation may be rewritten as:

$$\frac{\partial}{\partial x_j}(\rho u_i T) = \frac{\partial}{\partial x_j}\left[(\Gamma + \Gamma_t)\frac{\partial T}{\partial x_j}\right] \quad (10)$$

Where Γ and Γ_t, in Eq. (10), are the molecular and turbulent thermal diffusivity, respectively. The unknown turbulent thermal diffusivity Γ_t must be modelled in order to solve the energy equation and correspondingly to determine the characteristics of turbulent heat transfer problems. In zero equation model for the scalar field, an analogy is assumed tacitly between turbulent heat and momentum transfer. In such model, the unknown turbulent thermal diffusivity for heat Γ_t is expressed by the known turbulent viscosity μ_t, so that [17]:

$$\Gamma_t = \frac{\mu_t}{Pr_t} \quad (11)$$

Where Pr_t is the turbulent Prandtl number in which has given the value of 0.85 [19].

The different effective thermo-physical properties such as the density, specific heat, thermal conductivity, and dynamic viscosity of the nanofluid were defined by Williams et al. [20] as follows:

$$\rho_{nf} = (1 - \varphi)\,\rho_{bf} + \rho_P \varphi \quad (12)$$

$$C_{nf} = \left[\varphi\,(\rho\,C)_P + (\rho\,C)_{bf}\,(1 - \varphi)\right]/\rho_{nf} \quad (13)$$

$$\lambda_{nf} = (1 + 4.5503\,\varphi)\,\lambda_{bf} \quad (14)$$

$$\mu_{nf} = \exp(4.91\,\varphi/(0.2092 - \varphi))\,\mu_{bf} \quad (15)$$

In Eqs (12 – 15), the subscripts nf, bf and P denote the nanofluid, base fluid and particle, respectively. On the other hand, the base fluid thermo-physical properties such as density, thermal conductivity, and dynamic viscosity have been fitted as polynomial functions in temperature (Kelvins) using Engineering Equation Solver (EES) and are written in the following forms:

$$\rho_{bf} = 2813.77 \times 10^{-1} + 6351.93 \times 10^{-3}\,\mathrm{T} - 1761.03 \times 10^{-5}\,T^2 + 1460.96 \times 10^{-8}\,T^3 \quad (16)$$

$$\lambda_{bf} = -1056.42 \times 10^{-3} + 1011.33 \times 10^{-5}\,\mathrm{T} - 1772.74 \times 10^{-8}\,T^2 + 7994.88 \times 10^{-12}\,T^3 \quad (17)$$

$$\mu_{bf} = 9684.22 \times 10^{-5} - 821.53 \times 10^{-6}\,\mathrm{T} + 2345.21 \times 10^{-9}\,T^2 - 2244.12 \times 10^{-12}\,T^3 \quad (18)$$

These properties were used as user defined functions (UDF) subroutines and incorporated into Fluent 6.3 solver [16].

3. Numerical Scheme and Discretization

3.1. Computational Domain

It is assumed that the fluid phase and nanoparticles are in thermal equilibrium with zero relative velocity. This assumption may be considered realistic as nanoparticles are much smaller than microplarticles and the relative velocity decreases as the particle size decreases. Thus, the resultant mixture may be considered as a conventional single phase fluid [10]. Fig. 1 shows the considered geometrical configuration of the computational domain. It consists of a heated tube of 2819 mm length and 9.4 mm internal diameter [20]. Two adiabatic sections with 1000 mm and 500 mm lengths were positioned before and after the heated section. The considered nanofluid is a homogenous mixture composed of water and Al_2O_3 nanoparticles. The flow field is assumed to be axisymmetric with respect to the horizontal plane parallel to the tube axis.

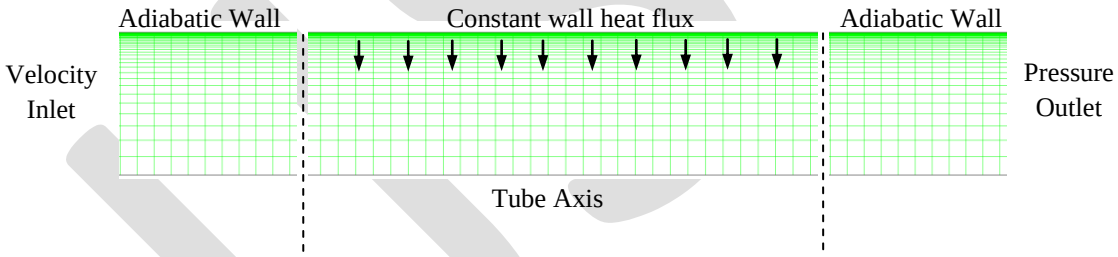

Fig.1. Schematic of the configuration of computational domain

3.2. Boundary Conditions and Grid System

The governing equations of the fluid flow are nonlinear and coupled partial differential equations. Inlet velocity and pressure outlet boundary conditions were, respectively, imposed at the inlet and outlet sections of the tube. No-slip conditions for velocity components and zero normal pressure gradients were set as the boundary conditions for solid wall. The boundary values for the turbulent quantities near the wall are specified using the two layers enhanced wall treatment functions [16]. It must be mentioned here that, only half of the tube was modelled due to the symmetry. In order to ensure fully developed turbulent flow at the entry of the tube section, an additional adiabatic tube length of 1000 mm is modelled along with the main tube length of 2819 mm. The computational domain was discretized using

structured non-uniform rectangular cells. By employing a nonuniform grids scheme, as shown in Fig. 1, the mesh density near the wall is about five times that of the mesh density at the centre of the tube. Following a grid-independence solution test, the computational grid has an average mesh density of about 8 cells/mm^2.

3.3. Numerical Procedure of Solution

The conservation equations of mass, momentum, turbulent kinetc energy, dissipation rate of turbulence and energy, Eqs (1), (2), (6), (7), and (10), respectively, were solved by control volume approach. Control-volume technique converts the conservation equations to a set of linear algebraic equations that can be solved numerically. A second order upwind descritization scheme was used to interpolate the unknown cell interface values required for the modelling of convection terms. Coupling between velocity and pressure was resolved by using Semi Implicit Method for Pressure Linked Equations (SIMPLE) algorithm [21]. FLUENT 6.3 code [16] solves the linear systems resulting from discretization schemes. During the iteration process, the residuals were carefully monitored and converged solutions were considered when the following criterion for convergence is satisfied:

$$\max \left| \frac{\theta^{i+1}}{\theta^{i}} - 1 \right| < 10^{-7} \tag{19}$$

Where θ: u, k, ε, and T and i denotes the number of iterations.

4. Results and Discussions

4.1. Validation of the present computational model

In order to verify the validity of the present computational model for hydrodynamic and thermal fields calculations, the CFD results were compared with experimental measurements available for not only the conventional fluids but also for the nanofluids. For this purpose, the experimental results of both heat transfer coefficient and pressure loss of pure water carried out by Williams et al. [20] have been used for comparison. Moreover, the experimental data of both heat transfer coefficient and pressure loss of aluminium dioxide Al_2O_3 conducted by Williams et al. [20] with different nanoparticle concentrations. Figure 2a presents the predicted data and experimental results of heat transfer coefficient of pure water. It is obvious that the maximum error for the heat transfer coefficient of pure water was about +8 %. The predicted data of pressure loss are compared with the experimental results of Williams et al. [20] for pure water as shown in Fig. 2b. It is seen from Fig. 2b that a maximum error for pressure loss for pure water was about +7 %.

To render the computational model more general, the heat transfer coefficient and pressure loss of Al_2O_3-water nanofluid, at three values of nanoparticle volume concentration, namely; 0.9 %, 1.8 %, and 3.6 %, are shown in Fig. 3 (a and b). Maximum error of value +10 % was clearly seen between the predicted and measured heat transfer coefficient in Fig. 3a, while, a value of +20 % maximum error was observed in Fig. 3b between the predicted and measured results of pressure loss of Al_2O_3.

The simulated results of the normalized turbulent kinetic energy are compared with the experimental data of Laufer [22] and are shown in Fig. 4. With the exception of peak value, the simulated results of turbulent kinetic energy are in excellent agreement with the experimental data. In order to explore more cases of validations, further comparisons for the average velocity and turbulent viscosity are carried out to convince the suitability of the present computational model. The simulated mean velocity field is compared with the experimental data of Laufer [22] and is shown in Fig. 5. The general agreement is excellently in accord with the experimental data and with the well-known logarithmic velocity profile that is given as follows:

$$u^+ = \frac{1}{\kappa}\ln y^+ + B \tag{20}$$

where κ is Von Kármán constant and has a value of 0.4 and B = 5.5 [18].

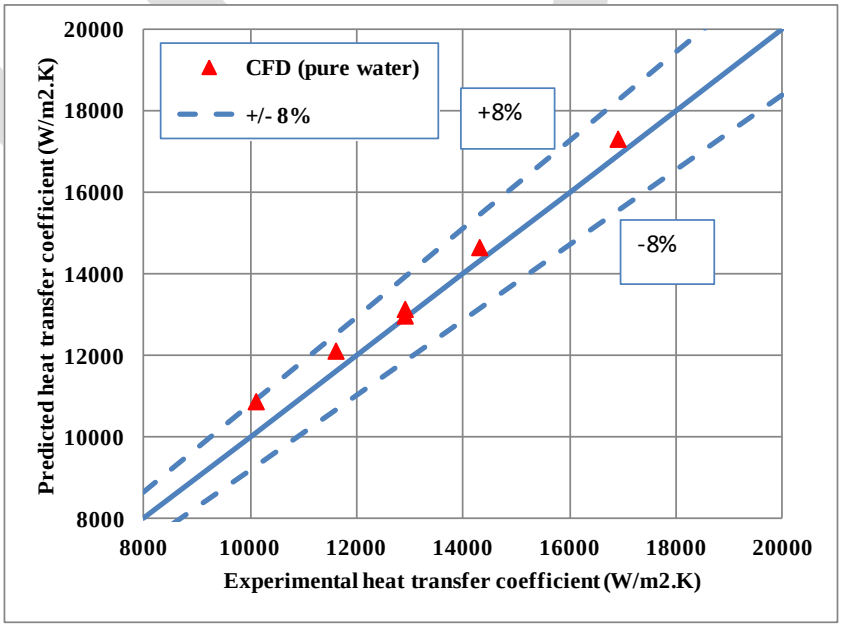

(a) Heat transfer coefficient

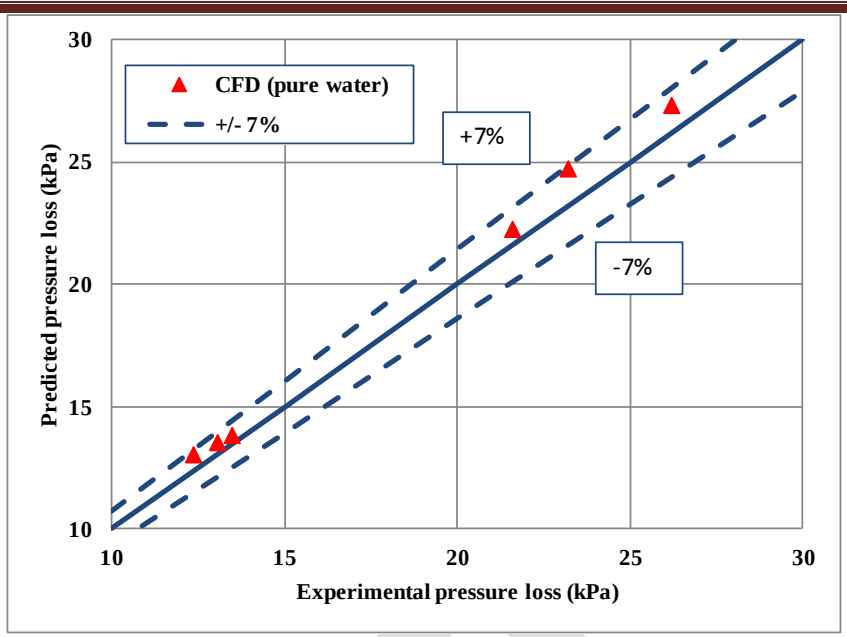

(b) Viscous pressure loss

Fig. 2. Validation of present CFD model against data measured by Williams et al. [20] for turbulent flow with heat transfer of pure water

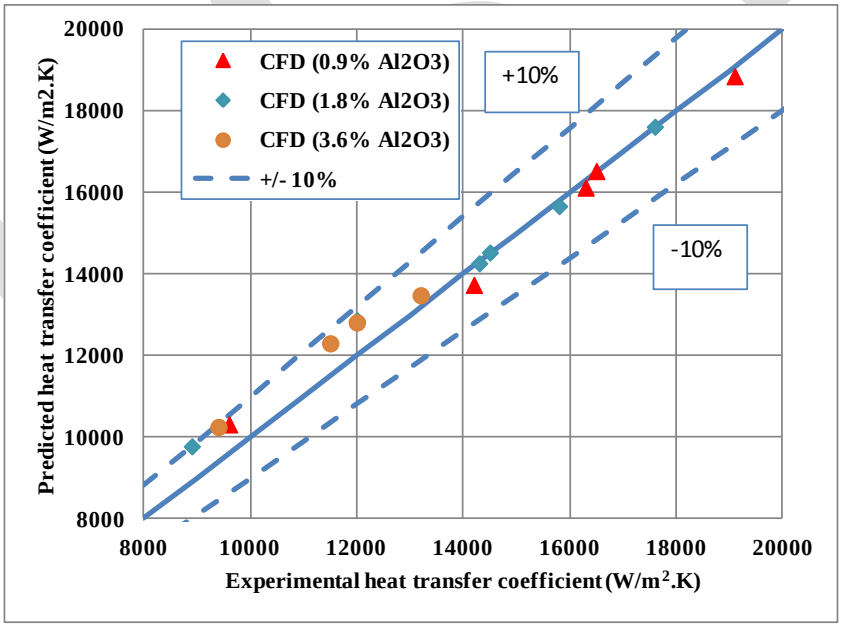

(a) Heat transfer coefficient

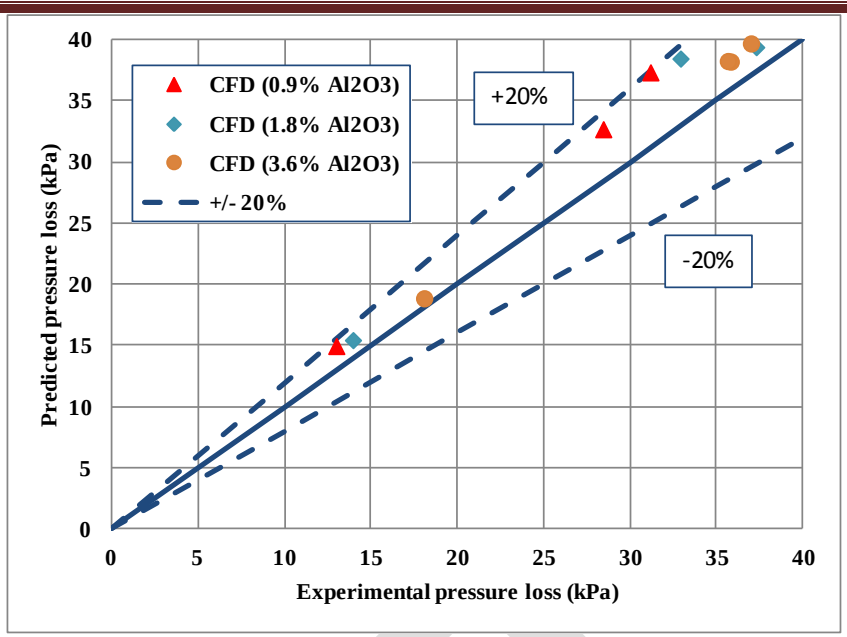

(b) Viscous pressure loss

Fig. 3. Validation of present CFD model against data measured by Williams et al. [20] for turbulent flow of Al_2O_3-water nanofluid with heat transfer

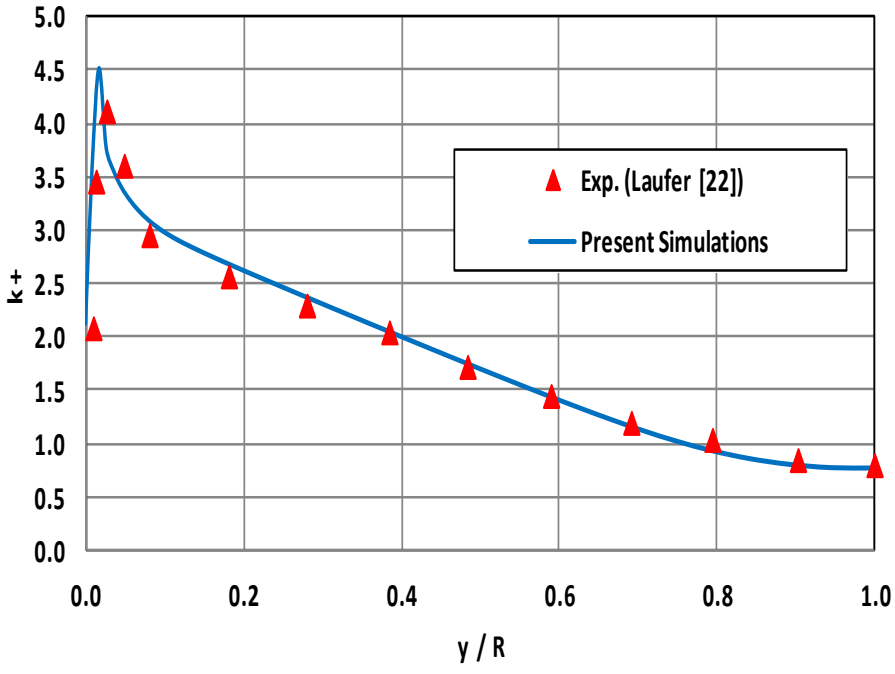

Fig. 4. Comparison of turbulent kinetic energy profiles for isothermal turbulent flow of pure water at Re = 40,000

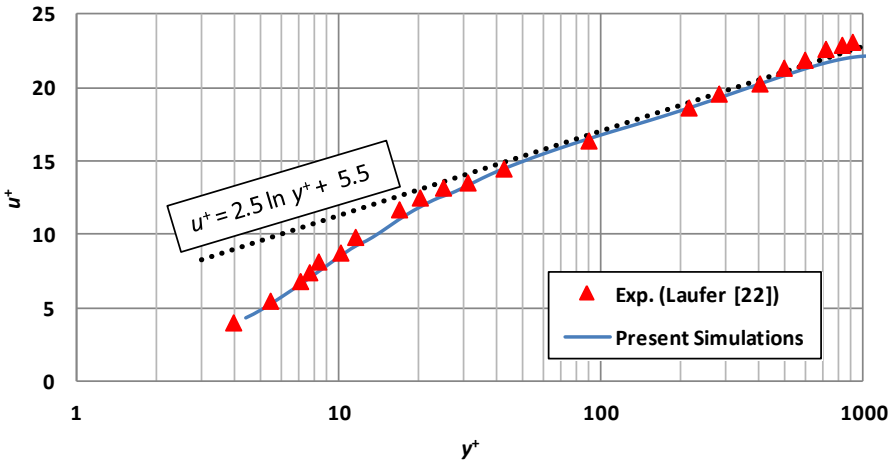

Fig. 5. Comparison of mean velocity profiles for isothermal turbulent flow of pure water at Re = 40,000

4.2. Application of the present computational model

After the above five comparisons and confirming that the present computational model is generating correct results in both hydrodynamic and thermal fields in case of not only pure water but also Al_2O_3-water with different volume concentrations. The predicted results of fully developed radial temperature (local temperature – inlet temperature) distribution at different values of volumetric concentrations ranging from 0 % (pure water) to 4.5 % are shown in Fig. 6. By increasing the volume concentration of nanoparticles, the radial temperature difference decreases and that is attributed to thickening the thermal boundary layer through the pipe.

The calculated results of wall shear stress of Al_2O_3-water flowing through pipe at constant wall heat flux of q = 50 kW/m^2 under turbulent flow regime with Re = 40000 at different values of volume concentrations are shown in Fig. 7. One easily seen that, as the volume concentration of nanoparticles increased, the wall shear stress increased due to increasing the dynamic viscosity of nanofluid.

The predicted results of average heat transfer coefficient of Al_2O_3-water flowing through pipe at constant wall heat flux q = 50 kW/m^2 under turbulent flow regime with Re = 40000 at different values of volume concentrations are shown in Fig. 8. As clearly seen in Fig. 8, the average heat transfer coefficient increased by increasing the volume concentration of nanoparticles and the reason is attributed to increasing the thermal boundary layer as already discussed in Fig. 6.

To better visualize the hydrodynamic characteristics in case of associated with heat transfer, the turbulent kinetic energy k and its dissipation rate ε are analyzed. Therefore, the distributions of both production rate and dissipation rate of turbulent kinetic energy k of Al_2O_3-water flowing through pipe with constant wall heat flux q = 50 kW/m^2 and without heat flux under turbulent flow regime with Re = 40000 at different values of volume concentrations are shown in Figs. 9 and 10. What has to be noticed form both figures is that there are no changes in both the production rate and dissipation rate of k in case of constant heat flux of value q = 50 kW/m^2 and without heat flux as well. This means that the temperature or the heat flux has passive effect on the hydrodynamic field characteristics, as demonstrated in [23] for low values of wall heat flux. On the other hand, with increasing the volume concentration of nanoparticles, the production rate and dissipation rate of k are increased and that is agreed quite well with the findings of Youssef et al. [24] in their recent article.

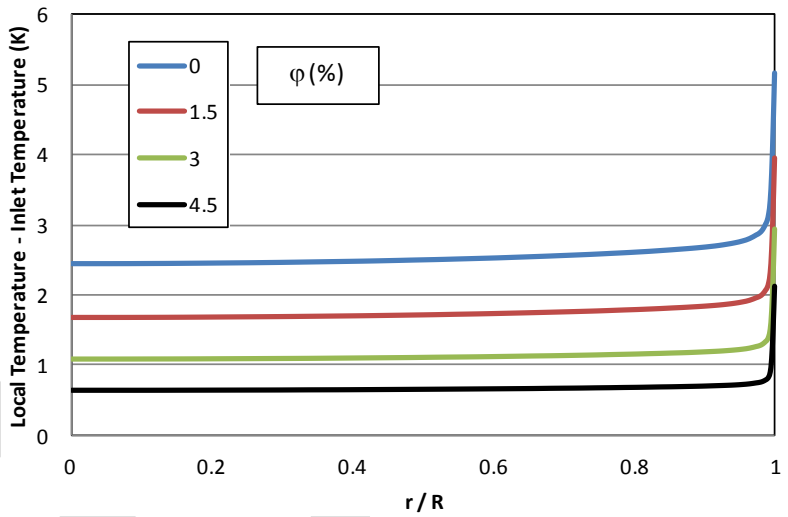

Fig. 6. Comparison of fully developed radial temperature distribution (local temperature – inlet temperature) at different values of volume concentration of Al_2O_3

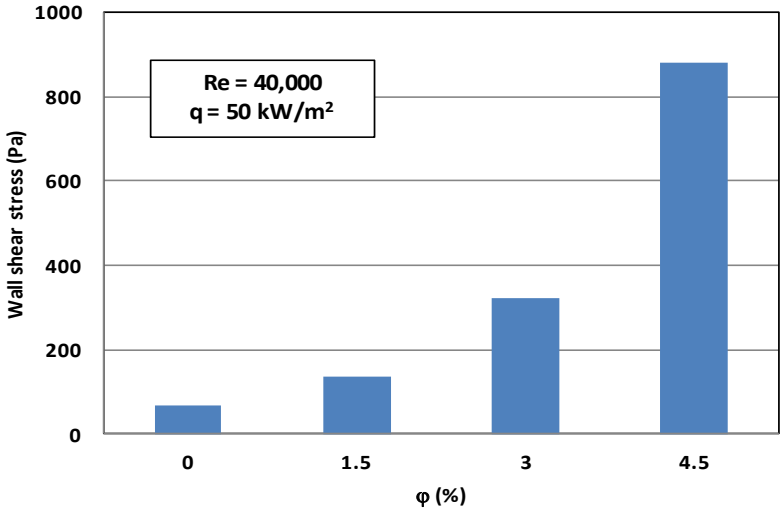

Fig. 7. Comparison of wall shear stress at different values of volume concentration of Al_2O_3

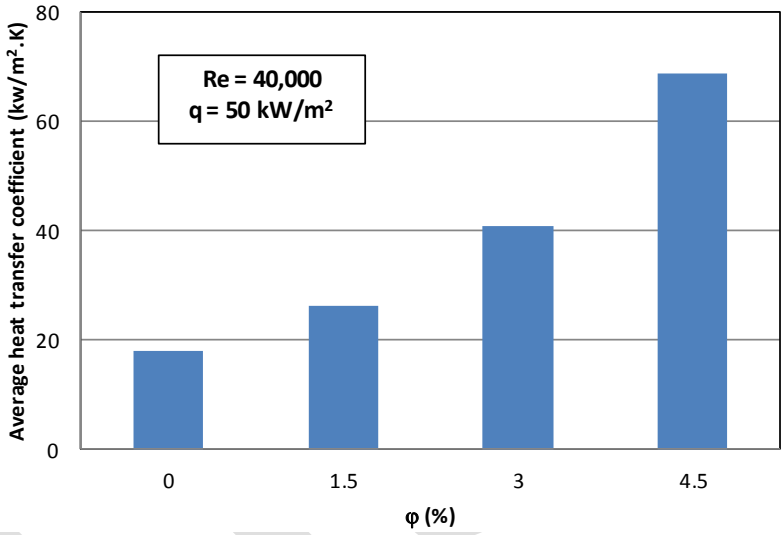

Fig. 8. Comparison of average heat transfer coefficient at different values of volume concentration of Al_2O_3

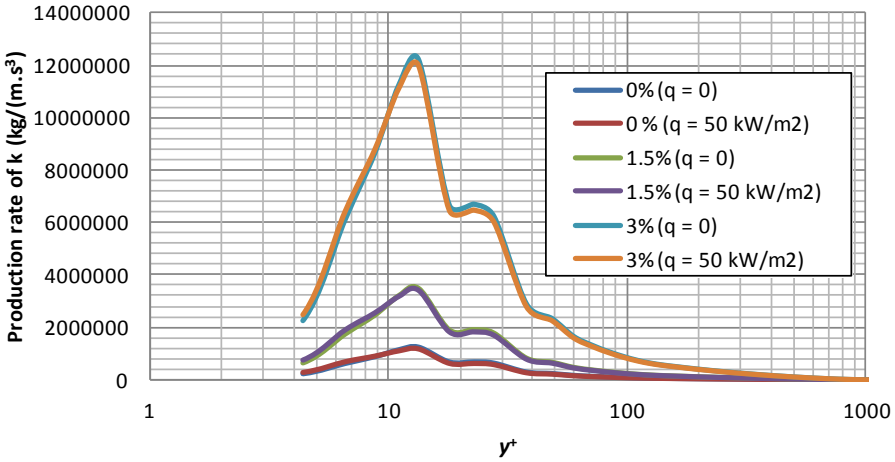

Fig. 9. Comparison of production rate of k with and without heat transfer at different values of volume concentration of Al_2O_3

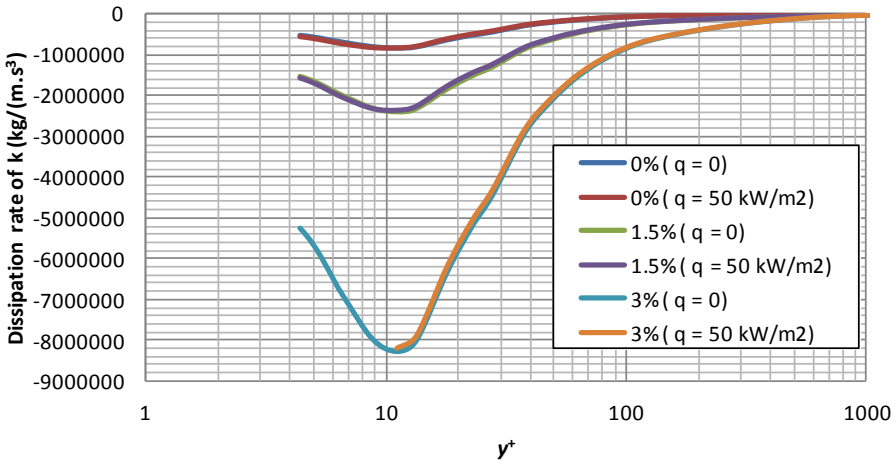

Fig. 10. Comparison of dissipation rate of k with and without heat transfer at different values of volume concentration of Al_2O_3

5. Conclusions

In this study, the thermal field characteristics of Al_2O_3-water nanofluid flowing in a circular tube under turbulent flow regime with and without heat transfer were numerically investigated. A single phase fluid model in conjunction with a two-equation turbulence model for hydrodynamic field and a zero-equation model for thermal field were employed to determine the different turbulent quantities of pure water and Al_2O_3-water with three nanoparticle volume concentrations. The computational model used in this study for hydrodynamic and thermal fields' calculations has been validated and proved its reliability for not only the conventional fluids but also the nanofluids. It was revealed from the simulated results that by increasing the volume concentration of nanoparticles, the radial temperature difference was decreased. This was attributed to the increase in the average heat transfer coefficient and the wall shear stress. Moreover, the predicted results showed that the temperature or the wall heat flux had passive effect on the hydrodynamic field characteristics. Ultimately, with increasing the volume concentration of nanoparticles, the production rate and dissipation rate of k were increased and that is agreed quite well with the previous studies.

Acknowledgments

The authors gratefully acknowledge the financial support provided by the Taif University, Saudi Arabia under Research Project No. 1- 434- 2383.

References

1. C. T. Nguyen, G. Roy, C. Gauthier, and N. Galanis "Heat transfer enhancement using Al_2O_3-water nanofluid for an electronic liquid cooling system," *Applied Thermal Engineering, Vol. 27, pp. 1501-1506, 2007.*
2. M. H. Kayhani, H. Soltanzadeh, M. M. Heyhat, M. Nazari, and F. Kowsary "Experimental study of convective heat transfer and pressure drop of TiO_2/water nanofluid," *International Communications in Heat and Mass Transfer, Vol. 39, pp. 456-462, 2012*.
3. A. A. Abbasian Arani, and J. Amani "Experimental study on the effect of TiO_2-water nanofluid on heat transfer and Pressure drop," *Experimental Thermal and Fluid Science, Vol. 42, pp. 107-115, 2012.*
4. W. Duangthongsuk and S. Wongwises "An experimental study on the heat transfer performance and pressure drop of TiO_2-water nanofluids flowing under a turbulent flow regime," *International Journal of Heat and Mass Transfer, Vol. 53, pp. 334-344, 2010.*
5. W. Duangthongsuk and S. Wongwises "Heat transfer enhancement and pressure drop characteristics of TiO_2-water nanofluid in a double-tube counter flow heat exchanger," *International Journal of Heat and Mass Transfer, Vol. 52, pp. 2059-2067, 2009.*
6. Y. He, Y. Jin, H. Chen, Y. Ding, D. Cang, and H. Lu "Heat transfer and flow behavior of aqueous suspensions of TiO_2 nanoparticles (nanofluids) flowing upward through a vertical pipe," *International Journal of Heat and Mass Transfer, Vol. 50, pp. 2272-2281, 2007.*
7. A. R. Sajadi, and M. H. Kazemi "Investigation of turbulent convective heat transfer and pressure drop of TiO_2/water nanofluid in circular tube," *International Communications in Heat and Mass Transfer, Vol. 38, pp. 1474-1478, 2011.*
8. S. M. Fotukian and M. N. Esfahany "Experimental study of turbulent convective heat transfer and pressure drop of dilute CuO/water nanofluid inside a circular tube," *International Communications in Heat and Mass Transfer, Vol. 37, pp. 214-219, 2010.*
9. M. H. Fard, M. N. Esfahany, and M. R. Talaie "Numerical study of convective heat transfer of nanofluids in a circular tube two-phase model versus single-phase model," *International Communications in Heat and Mass Transfer, Vol. 37, pp. 91-97, 2010.*
10. P. K. Namburu, D. K. Das, K. M. Tanguturi, and R. S. Vajjha "Numerical study of turbulent flow and heat transfer characteristics of nano fluids considering variable properties," *International Journal of Thermal Sciences, Vol. 48, pp. 290-302, 2009.*

11. S. Kondaraju, E. K. Jin, and J. S. Lee "Direct numerical simulation of thermal conductivity of nanofluids: The effect of temperature two-way coupling and coagulation of particles," *International Journal of Heat and Mass Transfer, Vol. 53, pp. 862-869, 2010.*

12. R. Lotfi, Y. Saboohi, and A. M. Rashidi "Numerical study of forced convective heat transfer of nanofluids: Comparison of different approaches," *International Communications in Heat and Mass Transfer, Vol. 37, pp. 74-78, 2010.*

13. M. E. Meibodi, M. Vafaie-Sefti, A. M. Rashidi, A. Amrollah, M. Tabasi, and H. S. Kalal "An estimation for velocity and temperature profiles of nanofluids in fully developed turbulent flow conditions," *International Communications in Heat and Mass Transfer, Vol. 37, pp. 895-900, 2010.*

14. H. Demir, A. S. Dalkilic, N. A. Kürekci, W. Duangthongsuk, and S. Wongwises "Numerical investigation on the single phase forced convection heat transfer characteristics of TiO_2 nanofluids in a double-tube counter flow heat exchanger," *International Communications in Heat and Mass Transfer, Vol. 38, pp. 218-228, 2011.*

15. V. Bianco, O. Manca, and S. Nardini "Numerical investigation on nanofluids turbulent convection heat transfer inside a circular tube," *International Journal of Thermal Sciences, Vol. 50, pp. 341-349, 2011.*

16. FLUENT 6.3 user guide, Fluent Inc., Lebanon, New Hampshire, 2005.

17. Y. Nagano and C. Kim "A Two-equation model for heat transport in wall turbulent shear flows", *ASME Journal of Heat Transfer, Vol. 110, pp. 583-589, 1988.*

18. Y. Nagano and M. Tagawa "An improved k-ε model for boundary layer flows", *ASME Journal of Fluids Engineering, Vol. 112, pp. 33-39, 1990.*

19. M. S. Youssef *"Near-wall modelling of turbulent flows with heat transfer"*, Ph. D. Dissertation, Nagoya Institute of Technology, Japan, 1994.

20. W. Williams, J. Buongiorno, and L. Hu "Experimental investigation of turbulent convective heat transfer and pressure loss of alumina/water and zirconia/water nanoparticle colloids (nanofluids) in horizontal tubes", *ASME Journal of Heat Transfer, Vol. 130, pp. xx – yy, 2008.*

21. S. V. Patankar *"Numerical Heat Transfer and Fluid Flow"*, Hemisphere Publishing Corporation, New York, 1980.

22. J. Laufer, "The structure of turbulence in fully developed pipe flow", NACA Report, Report number 1174, 1954.

23. L. Fulachier and R. Dumas "Spectral analogy between temperature and velocity fluctuations in a turbulent boundary layer", J. of Fluid Mechanics, Vol. 77, pp. 257-277, 1976.

24. M. S. Youssef, A-F. Mahrous, and E. B. Zeidan "Numerical investigationon hydrodynamic field characteristics for turbulent flow of water-TiO_2 nanofluid in a circular tube", *International Journal of Mechanical Engineering (IJME), Vol. 2, Issue 5, pp. 151 – 164, November 2013.*

Nomenclature

	Roman Symbols
C	Specific heat
$C_{\varepsilon 1}, C_{\varepsilon 2}, C_{\mu}$	Turbulence model coefficients
L_e	Characteristic length scale = $k^{3/2}/\varepsilon$
k	Turbulent kinetic energy = $\overline{u_i' u_j'}/2$
P	Average pressure
Pr_t	Turbulent Prandtl number
q	Wall heat fux
R	Pipe radius
T	Mean temperature
t	Fluctuating temperature
Re	Reynolds number
u	Mean velocity component in x direction
u'	Fluctuating velocity component in x direction
u_i'	Fluctuating velocity component in x_i direction
u_i	Mean velocity component in x_i direction
u_τ	Friction velocity = $\sqrt{\tau_w/\rho}$
v	Fluctuating velocity component in y direction
x, y	Coordinates
y	Wall distance
z	Axial coordinate

Greek Symbols

δ_{ij}	Kronecker's delta
ε	Dissipation rate of k
φ	Nanoparticle volume concentration
μ, μ_t	Dynamic, and turbulent viscosities
Γ, Γ_t	Molecular and turbulent kinematic eddy viscosities
λ	Thermal conductivity
κ	Von Kármán constant
ρ	Density
σ_k, σ_ε	Turbulent model constants for diffusion of k and ε
τ, τ_w	Time and wall stress tensor

Subscripts

bf	Base fluid
i, j, k	Index refers to spatial coordinates
nf	Nanofluid
P	Particles
t	Turbulent
w	Wall

Superscripts

+	Normalization by wall variables, i.e., u_τ for velocity, and u_τ^2 for k